

Combining state space demand modeling with design optimization for integrated energy systems planning

Yuan Huang¹, Jian Lin¹, Meina Xie¹, Nianyuan Wu¹, Shan Xie¹, Yingru Zhao^{1*}

¹ College of Energy, Xiamen University, Xiamen, China

ABSTRACT

Traditional energy planning is a one-way process from load forecasting to system optimisation, an approach that cannot support the increasing variability on both the supply and demand sides. This study proposes an energy simulation and system optimisation approach based on the state-space method for collaborative dynamic planning of the supply and demand sides of an integrated energy system. The case results show that taking into account the real-time dynamic characteristics of the load can improve the model accuracy; at the same time, system planning based on a synergistic supply and demand perspective can achieve overall optimality and rationalise the two-way interaction between the demand and supply sides.

Keywords: Dynamic modelling, state space method, collaborative supply and demand optimisation, energy system planning.

NONMENCLATURE

<i>Abbreviations</i>	
CTF	contrast transfer function
MILP	mixed integer linear programming
SSM	state space modeling
<i>Symbols</i>	
X Y F	conduction transfer functions
q_i q_o	internal and external surface heat fluxes
T	temperature

1. INTRODUCTION

The World Energy Development Report 2020 points out that global energy is undergoing an accelerated transformation towards efficient, clean and diversified features, and that the global energy supply and demand pattern is entering a phase of profound adjustment. The mismatch between the supply and demand systems of various sectors has led to a structural imbalance between supply and demand in the energy sector. On the supply side, there are problems such as unbalanced distribution of resources and high volatility of renewable energy, while on the demand side, energy consumption remains high, concentrated in three major areas: industry, transportation and construction[1], especially in buildings, where energy consumption is rising sharply along with the continuous rise in the total building stock and the improvement of living comfort. Energy consumption in the building sector accounts for more than one-fifth of the end-use energy consumption of society as a whole[2], with heat loss from heat transfer in the envelope accounting for about 70% or more of the energy loss in buildings[3].

In response to the increasing variability on both the supply and demand sides, integrated energy systems with collaborative supply and demand planning have emerged. At present, in order to improve the efficiency of new energy utilisation, the study of building a multi-energy synergistic optimisation strategy model for integrated energy systems on both the supply and demand sides, taking into account the influential roles between the supply side, demand side and energy conversion, is still a hot and cutting-edge topic of research for scholars in this field. There are two main ways of thinking when existing research methods deal with the integrated energy system planning problem of supply and demand synergy. One is to start from the

perspective of energy sector planning[4][5], and the calculation and simulation of building energy consumption is relatively crude, without considering the factor of heat storage in the envelope structure changing with time, which leads to large errors in the building load results caused by this part and affects the actual operation effect of the system. Another way of thinking is that both demand-side load simulation and supply-side energy system simulation are done based on simulation tools[6]. This approach to system optimisation can only be done by comparing each alternative through multiple simulations, which is computationally expensive and cannot traverse all feasible solutions at once to find the global optimal solution.

Based on the above reasons, this paper proposes a state space method (SSM) for dynamic demand modelling and co-optimisation of integrated energy systems. The state space method is a dynamic simulation method that is continuous in time and discrete in space. Based on the state space model, the dynamic equations of the system can be obtained in a simple form with clear physical meaning and can be solved with high speed and accuracy. The research framework of this paper is shown in Figure 1. Firstly, based on the state space method, the dynamic simulation of the baseline energy demand of an old community-based youth flat is carried out, and a passive energy retrofit strategy with different levels of gradients of the building envelope on the demand side of the integrated system is designed. Secondly, a variety of renewable energy supply and storage technologies are introduced to achieve active energy savings from the supply side. The system design and dispatching strategy is optimised with economic and environmental objectives in mind to determine the best overall energy saving strategy and optimal equipment configuration from a supply and demand synergy planning perspective.

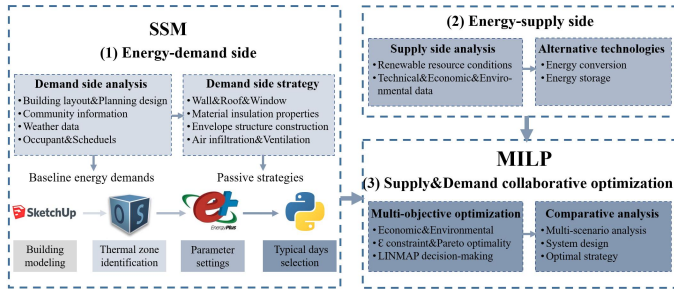


Fig 1 Schematic of the holistic approach.

2. METHODS

2.1 State space model

The thermal characteristics of the unsteady heat transfer from the demand-side building envelope are represented by the transfer function coefficients, which are the basic data for modelling and analysing the annual energy consumption of a building. This paper calculates the transfer function coefficients based on the state-space principle of modern control theory, and converts the effect of thermal disturbances on indoor air temperature into a series of heat transfer characteristic parameters, on the basis of which the calculation of the building room temperature and the annual baseline load of the community is carried out. The building can be considered as a thermal system consisting of the envelope and the indoor air, therefore the load calculation model can be divided into a zone air heat transfer calculation model and an envelope heat transfer calculation model.

The regional air heat transfer calculation model consists of the equations for the internal and external surface balance of the building, the building body heat balance and the indoor air heat balance.

$$C_z \frac{dT_z}{dt} = \sum_{i=1}^{N_{si}} \dot{Q}_i + \sum_{i=1}^{N_{surfaces}} h_i A_i (T_{si} - T_z) + \sum_{i=1}^{N_{zones}} \dot{m}_i c_p (T_{si} - T_z) + \dot{m}_{inf} c_p (T_{\infty} - T_z) + \dot{Q}_{sys} \quad (1)$$

where $C_z \frac{dT_z}{dt}$ is the rate of change of heat storage in the area air with time; $\sum_{i=1}^{N_{si}} \dot{Q}_i$ is the load from convection of internal heat sources such as personnel and equipment; $\sum_{i=1}^{N_{surfaces}} h_i A_i (T_{si} - T_z)$ is the convection heat exchange between the envelope structures heat transfer; $\sum_{i=1}^{N_{zones}} \dot{m}_i c_p (T_{si} - T_z)$ is the air mixing heat transfer in the area; $\dot{m}_{inf} c_p (T_{\infty} - T_z)$ is the heat transfer from air infiltration; $\dot{Q}_{sys} = m_{sys} c_p (T_s - T_z)$ is the heat transfer due to the ventilation system.

The envelope heat transfer calculation model is based on the contrast transfer function (CTF) method[7], which characterises the thermal response of the envelope material, as in equation (2).

$$q''_{i,t} = \sum_{m=1}^M X_m T_{i,t-m+1} - \sum_{m=1}^M Y_m T_{o,t-m+1} + \sum_{m=1}^k F_m q''_{i,t-m} \quad (2)$$

where k is the order of the conduction transfer function, M is a finite number defined by the order of the conduction transfer function and X , Y and F are the CTF coefficients of the building envelope. This transient heat transfer equation is expressed as a state space equation to solve for the transfer function coefficients:

$$\begin{bmatrix} \frac{dT_1}{dt} \\ \frac{dT_2}{dt} \end{bmatrix} = \begin{bmatrix} -\frac{1}{RC} - \frac{hA}{C} & \frac{1}{RC} \\ \frac{hA}{C} & -\frac{1}{RC} - \frac{hA}{C} \end{bmatrix} \begin{bmatrix} T_1 \\ T_2 \end{bmatrix} + \begin{bmatrix} \frac{hA}{C} & 0 \\ 0 & \frac{hA}{C} \end{bmatrix} \begin{bmatrix} T_o \\ T_i \end{bmatrix} \quad (3)$$

$$\begin{bmatrix} q''_i \\ q''_o \end{bmatrix} = \begin{bmatrix} 0 & -h \\ h & 0 \end{bmatrix} \begin{bmatrix} T_1 \\ T_2 \end{bmatrix} + \begin{bmatrix} 0 & h \\ -h & 0 \end{bmatrix} \begin{bmatrix} T_o \\ T_i \end{bmatrix} \quad (4)$$

where $R = \frac{l}{kA}$; $C = \frac{\rho c_p l A}{2}$ (l is the thickness; A is the surface area exposed to ambient temperature); h is the convective heat transfer coefficient on both sides of the wall; T_o is the outdoor temperature; T_i is the indoor temperature; and the two surface heat fluxes (q''_i and q''_o) are the output variables. Based on this, the heat transfer problem for a multi-storey uniform envelope can be solved. Finally, the outdoor weather model is chosen and the heat transfer balance equation for the area air and the heat transfer balance equation for the envelope can be solved to calculate the building cooling and heating loads.

2.2 Integrated optimisation model

The system schematic of the collaborative planning model constructed in this study incorporating the energy supply and demand characteristics of the community is shown in Figure 2. In this paper, an optimisation model for collaborative planning is constructed through mixed integer linear programming (MILP). The material-energy balance of each energy stream in the collaborative planning model and the operational constraints are first modelled, and then the design and operation of the system are optimised with multi-objectives by combining economic and environmental indicators.

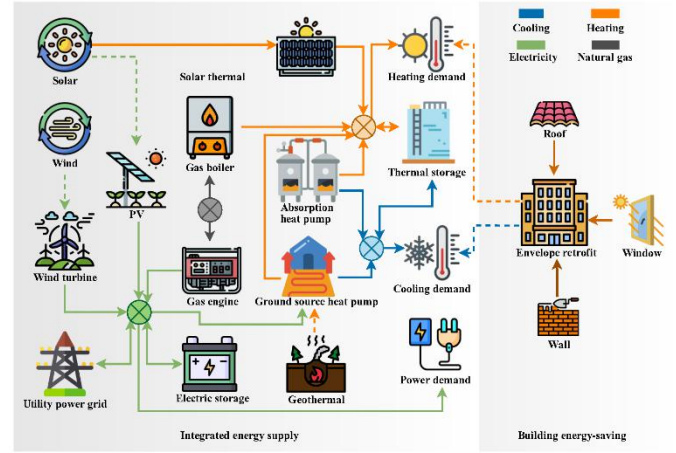


Fig 2 Schematic diagram of the energy system.

The energy balance is the basic constraint for coupling the modules of the energy centre to achieve multi-energy complementarity and matching supply and demand. The energy conversion balance of the energy producing equipment is shown in equation (5),

$$E_{e,i,msp,d,h}^{In} \times \eta_{e,e',i,msp,d,h} = E_{e',i,msp,s,d,h}^{Out} \quad (\forall e, e', i, msp, s, d, h) \quad (5)$$

where the subscript msp denotes the capacity device and $\eta_{e,e',i,msp,d,h}$ represents the energy conversion efficiency or coefficient of performance associated with the input energy type e and the output energy type e' .

The energy balance of the energy storage devices for adjacent periods is as follows.

$$E_{e,i,mss,d,h}^{Sto} = E_{e,i,mss,d,h-1}^{Sto} + \eta_{e,i,mss,d,h}^{In} \times E_{e,i,mss,d,h}^{In} - \frac{E_{e,i,mss,d,h}^{Out}}{\eta_{e,i,mss,d,h}^{Out}} - E_{e,i,mss,d,h}^{Loss} \quad (\forall e, i, mss, d, h) \quad (6)$$

where $E_{e,i,mss,d,h}^{Sto}$ represents the storage level of the energy storage system mss at the end of time period h , $\eta_{e,i,mss,d,h}^{In}$ and $\eta_{e,i,mss,d,h}^{Out}$ represent the energy charging and releasing efficiency of the energy storage system respectively, and $E_{e,i,mss,d,h}^{Loss}$ is the stored energy loss of the energy storage system during time period h .

The main types of constraints considered to optimise the operation of the system include energy equipment capacity, load state and resource availability constraints. Equation 7 is the capacity constraint for each energy device.

$$CAP_{e,i,ms}^{In/Out} \times PL_{e,ms}^{Min} \times t_h \leq E_{e,i,ms,d,h}^{In} \leq CAP_{e,i,ms}^{Out} \times PL_{e,ms}^{Max} \times t_h \quad (\forall e,i,ms,d,h) \quad (7)$$

where $CAP_{e,i,ms}^{In/Out}$ represents the rated input or output power of the device, $PL_{e,ms}^{Min}$ and $PL_{e,ms}^{Max}$ are the maximum and minimum partial load factors for this type of device respectively. The state of charge of the energy storage system is constrained as follows.

$$CAP_{e,i,mss}^{Sto} \times SOC_{e,mss}^{Min} \leq E_{e,i,mss,d,h}^{Sto} \leq CAP_{e,i,mss}^{Sto} \times SOC_{e,mss}^{Max} \quad (\forall e,i,mss,d,h) \quad (8)$$

where $CAP_{e,i,mss}^{Sto}$ denotes the storage capacity of the energy storage device, $SOC_{e,mss}^{Min}$ and $SOC_{e,mss}^{Max}$ denote the minimum and maximum charge states allowed for the device respectively.

The renewable resource availability constraint includes a constraint on the amount of available unit resources (Equation 9), and a constraint on the available building space within the community (Equation 10).

$$E_{er,i,msr,d,h}^{In} \leq E_{er,i,d,h}^{Rene,Max} \quad (\forall er,i,msr,d,h) \quad (9)$$

$$\sum_{msr} CAP_{e,i,msr,rs} \times \theta_{msr,rs}^S \leq S_{i,rs}^{Max} \quad (\forall e,i,rs) \quad (10)$$

where $E_{er,i,d,h}^{Rene,Max}$ denotes the maximum amount of renewable energy er available per unit in community i at moment h , $S_{i,rs}^{Max}$ is the maximum space available in community i for the construction of the relevant technical facilities for the use of renewable energy rs , and $\theta_{msr,rs}^S$ is the space occupation factor of the renewable energy utilisation equipment msr .

The evaluation indicators involved in the case model include economic and environmental indicators. The total NPV cost consists of the investment cost $CAPEX_m$ for each technology option module on the supply and demand side of the system and the net present value of the annual operating costs over the project planning period, as in equation 11.

$$NPC = \sum_m CAPEX_m + \sum_y \frac{1}{(1+r)^y} \times \left[\sum_m MAEX_{m,y}^y + \sum_{eu} (EEX_{eu,y}^{Imp,y} - EIN_{eu,y}^{Exp,y}) \right] \quad (11)$$

where r is the discount rate, $MAEX_{m,y}^y$ is the annual maintenance expenditure associated with each technology module, and $EEX_{eu,y}^{Imp,y}$ and $EIN_{eu,y}^{Exp,y}$ are

the annual energy expenditure and revenue associated with energy purchases and sales respectively.

Total carbon emissions TCE is calculated based on the fossil energy consumed during the operation of the integrated energy system, where the public grid electricity carbon emissions are calculated based on an equivalent carbon emission factor related to the local grid electricity mix, expressed as follows.

$$TCE = \sum_{eu,y} E_{eu,y}^{Imp,y} \times \theta_{eu,y}^{ECE} \quad (12)$$

where $E_{eu,y}^{Imp,y}$ is the total annual input for each energy type and $\theta_{eu,y}^{ECE}$ is the corresponding equivalent carbon emission factor.

3. CASE STUDY

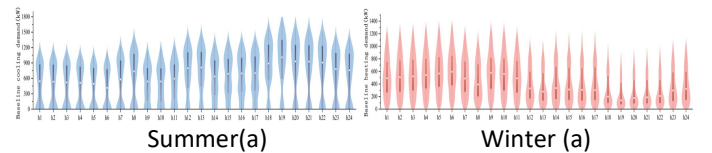
This study is based on a case study of an integrated energy system retrofit project for an old community-based youth apartment complex located in Shanghai, China. The community has a floor area of 35,280m² and 10 apartment buildings. The community currently relies on the grid for its domestic electricity load and the heat load is provided by an old boiler, making it difficult to meet the growing energy load of the community. The demand-side load simulation model was built on the Energyplus platform.

Table 1

Demand-side energy efficiency retrofit strategies

Energy saving retrofit items	Retrofit levels	Structural heat transfer coefficient (W/(m ² ·K))	Cost (including materials and labor costs, RMB/m ²)
Exterior wall retrofit	A1	0.824	47.316
	A2	0.518	55.392
	A3	0.151	130.592
Roof retrofit	B1	0.737	94.936
	B2	0.500	74.136
	B3	0.182	150.936
Window retrofit	C1	3.492	200
	C2	2.2	256
	C3	0.85	280

(The level of energy-saving retrofit increases with the strategy number.)



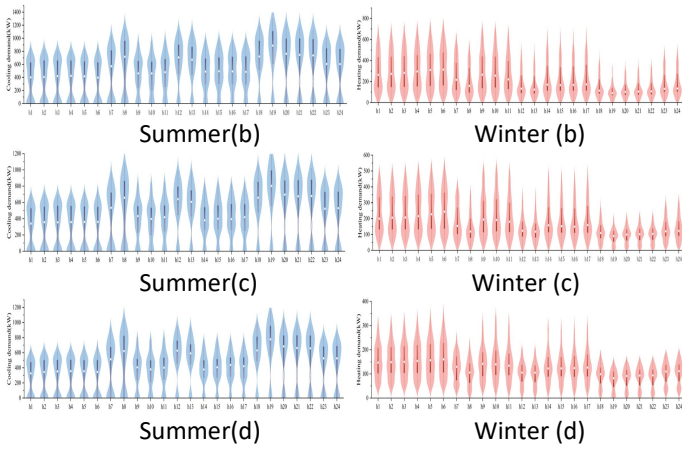


Fig 3 Violin diagrams for the baseline scenario(a), primary(b), intermediate(c) and advanced(d) retrofit strategies with hour-by-hour loads throughout the year.

4. RESULTS AND DISCUSSION

According to the relevant parameters set in the Shanghai Design Standard for Energy Efficiency of Residential Buildings, the first is the demand-side building energy efficiency retrofit as shown in Table 1, which is designed for different performance gradients for external walls, roofs and external windows, respectively. Violin plots of the annual hour-by-hour cooling and heating load simulation results for the baseline scenario, the lowest level retrofit strategy, the compromise retrofit strategy and the highest level retrofit strategy are given here. As shown in Figure 3, compared to the annual energy demand levels in the baseline scenario, the retrofit scenarios show a significant reduction in both heating and cooling demand throughout the year, with the higher the level of the retrofit strategy the greater the load reduction.

The analysis of the system optimisation model solution for collaborative supply and demand planning, after the optimisation model solution, the set of economic and environmental dual-objective optimisation solutions of the system can be plotted as a Pareto curve, as shown in Figure 4.

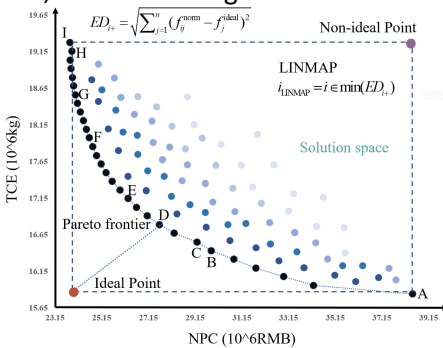


Fig 4 Pareto frontier for multi-objective optimization.

As can be seen from Figure 4, there are certain trade-offs between the two objectives. Points F, A and C in the diagram are the economically optimal, environmentally optimal and integrated optimal solutions respectively. The integrated optimal solution is obtained according to the Linear Programming Techniques for Multidimensional Analysis of Preference (LINMAP) decision making method, where the annualised cost and average annual carbon emissions of the system are moderate and the system has the best overall efficiency. Figure 5 shows the comparison of the economic and environmental indicators of the six representative optimal solutions on the Pareto front and the baseline scenario respectively. Compared to the baseline scenario, the optimised economically optimal scenario reduces costs by 24% and emissions by 40%, and the environmentally optimal scenario reduces emissions by 50%.

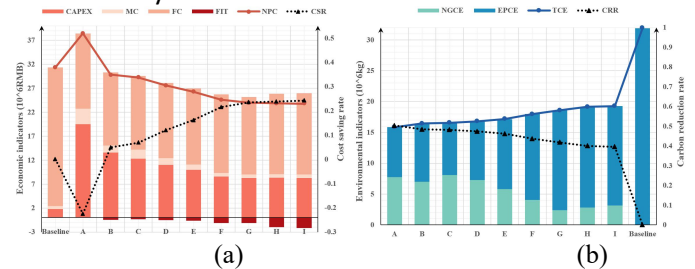


Fig 5 Comparison of economic(a) and environmental(b) indicators for the representative optimal solution and the baseline scenario.

There are significant differences in the design options for different scenarios of the system. As shown in Figure 6, (a) and (b) are the economic optimal scenario and the carbon emission optimal scenario for the system without demand-side retrofitting, respectively; (c) is the economic optimal scenario and the low retrofit cost scenario (50% reduction in demand-side retrofit cost); and (d) is the optimal scenario and the low carbon scenario (50% reduction in carbon emission). The system design parameters for different optimal solutions vary greatly, so the supply and demand co-programming model proposed in this paper gives different design scenarios for different optimization objectives, and trade-offs can be made among the different scenarios according to actual needs.

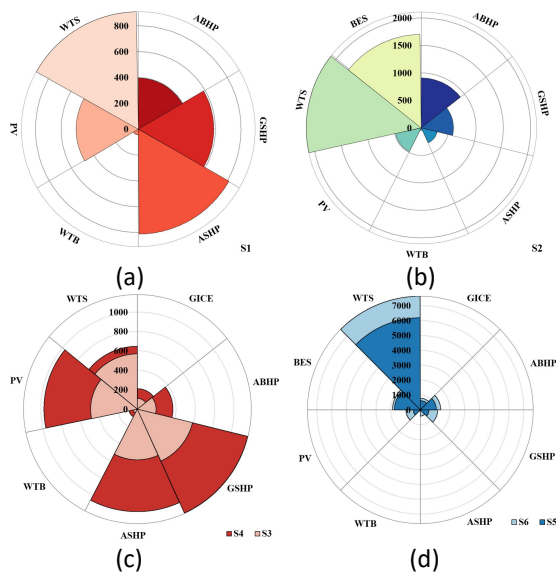


Fig 6 Nightingale rose diagram for different scenarios of installed capacity configurations.(Energy production equipments unit: kW; Energy storage equipments unit: kWh)

5. CONCLUSIONS

This paper verifies the validity of the model through case studies, and the optimisation results show a significant improvement in the overall performance and efficiency of community energy efficiency and emission reduction. Exploring the holistic planning and operation of integrated energy systems with such a forward-looking perspective and systemic thinking can better assess the energy saving and emission reduction potential of demand-side retrofitting and bring into play the flexible value of the demand side, in which the energy and information flows flow in both directions in an orderly manner to promote the overall balance of the energy supply and demand system in an interactive and mutually co-ordinated process. At the same time, it is important to consider the real-time dynamic characteristics of loads during system optimisation and design to improve the accuracy of building load modelling and forecasting, thus enabling better decision-making on effective solutions to meet system-level energy demand.

ACKNOWLEDGEMENT

The authors are grateful for the support from National Natural Science Foundation of China under grant No. 51876181. The work is also supported by the Youth Innovation Fund of Xiamen, China with grant No. 3502Z20206034.

REFERENCE

- [1]Du WC, Xia XH. How does urbanization affect GHG emissions? A cross-country panel threshold data analysis. *Appl Energy* 2018;229:872–83.
- [2] International Energy Agency. *World Energy Outlook 2018*;2018. <https://webstore.iea.org/world-energy-outlook-2018>.
- [3]Rodríguez-Soria B, Domínguez-Hernández D,Pérez-Bella J,Coz-Díaz J.Review of international regulations governing the thermal insulation requirements of residential buildings and the harmonization of envelope energy loss. *Renewable and Sustainable Energy Reviews* 2014;34:78-90.
- [4]Jing R, Kuriyanb K, Lin J, et al. Quantifying the contribution of individual technologies in integrated urban energy systems – A system value approach. *Appl Energy*. 2020, 266:114859.
- [5]Zheng XY, Qiu YW, Zhan XY, et al. Optimization based planning of urban energy systems: Retrofitting a Chinese industrial park as a case-study. *Energy*. 2017, 139: 31-41.
- [6]Zhang W, Valencia A, Gu L, et al. Integrating emerging and existing renewable energy technologies into a community-scale microgrid in an energy-water nexus for resilience improvement. *Appl Energy*.2020, 279:115716.
- [7]Vera S,Pinto C, Tabares-Velasco P, Bustamante W.A critical review of heat and mass transfer in vegetative roof models used in building energy and urban environment simulation tools. *Appl Energy* 2018;232:752-764.